Click to see poster presentation

[PS]Naturally Fractured Granite and Volcanic Basement Rock Formation Evaluation in Neuquén Basin, Argentina*

Martin Paris[1], Marcelo Barrionuevo[2], Carlos Palacios[2], Guillermo Crespo[1], Juan Grisolia[1], and Claudio Rabe[1]

Search and Discovery Article #11292 (2020)**
Posted January 20, 2020

*Adapted from extended abstract based on poster presentation given at 2019 International Conference and Exhibition, Buenos Aires, Argentina, August 27-30, 2019
 DOI:10.1306/11292Paris2020

[1]BHGE, Buenos Aires, Argentina (martin.paris@bhge.com)
[2]YPF S.A., Buenos Aires, Argentina

Abstract

Understanding a naturally fractured rock network is a challenge. Understanding granitic and volcanic petrophysics is another challenge. Consequently, a fractured reservoir in a basement rocks is a double challenge. The Guanaco Field is in the Neuquén province, West Argentina. Its “wet or dry” gas production comes from basement rocks. Fractures that are present in these rocks allow the storage and permeability to fluid flows, but the fracture intensity is highly variable. For this reason, productivity is highly variable from one well to another. This heterogeneity is also noticeable along the section of vertical wells. Consequently, completions must be selective. Detailed formation evaluation is the key for a successful completion. This paper describes a case study that integrates data from mudlogging, open hole logs and a 3D static model to design a completion strategy. Borehole imaging logs (from wireline resistivity and acoustic) are the main technologies to characterize the fracture network. This data integration enabled selection of the best potential intervals to perforate and stimulate. Although these are naturally fractured reservoirs, a hydraulic fracture must be performed to start production. Well testing and production logging confirm the results of this methodology.

Introduction

The basement hydrocarbon potential has been investigated in several places of the Huincul Dorsal since the beginning of the development of the region. Many zones are gas and oilfields among them Guanaco Field. The Guanaco structure is located in the center-south of the Al Norte de la Dorsal concession (Figure 1), generated by different orogenies that act in the basin against the most important morphostructural element, such as the Dorsal de Huincul, where basement faults suffer different reactivations (Figure 2). Gas reserves have already been proven in this structure, with some good-producing wells reaching production above 100 Mm^3/day in the eastern part of the structure. The eastern zone has

been drilled more than the western zone because the eastern zone has better hydrocarbon productions. A plan to evaluate the productivity of these deep objectives has been developed based on the intervention of old wells and drilling of wells in areas far from the most productive area.

Location and Background

Guanaco gas field is near Cutral Có city, 5 km to the north, and 110 km to the west of Neuquén City (Figure 1). The reservoir has an elongated shape in the direction east-west and follows the anticline geometry that defines the trap.

Geology and Petroleum System of the Study Area

The stratigraphic column of the study area (Figure 2) constitutes:

- Paleozoic granitoids and volcaniclastics deposits of the Precuyano Cycle.
- Siliciclastic deposits corresponding to the Cuyo Group.
- Clastic and carbonate deposits corresponding to the Lotena, Mendoza and Rayoso groups.
- Continental deposits of the Neuquén Group.

Two oil systems are considered that have contributed to charging the reservoirs in the studied area of Dorsal de Huincul. Vaca Muerta shale, located above Lotena Formation, is the source rock of oil at this area and the Molles shale is the source of dry gas. In this study the system constituted by Los Molles, PreCuyo and Basement are detailed.

Structural Framework

The studied area (north of the Dorsal) was a depocenter for the Precuyano and Cuyo Group. A hemigraben of east-west orientation was developed, with the block high towards the south, like a step of the Dorsal de Huincul. The initial stage of formation of the predominantly distensive basin was followed by a compressive stage with associated lateral displacement (Figure 3). The southern block behaved as a rigid block, and the northern block moved, generating structures of the "flower" type. The main structural tendency is WNW-ESE, showing an E-W trend to the south. In the north the structures show NNW-SSE orientation, developing zones of greater deformation that can be resolved in master faults, secondary faults and folds associated with them.

PreCuyo and Choiyoi in this Area

The Precuyo Cycle in the Guanaco structure is composed of effusive and explosive volcanic units. The effusive rocks are andesitic lavas and autobrecciated lavas. The explosive volcanic rocks are of rhyolitic composition. In well Gu-1093, 18 m of core are mainly autobrecciated lavas. From thin sections of cutting, the underlying volcaniclastic intercalation and the granodiorite were reconstructed (Figure 4). The core documents porosities of 1 to 12%.

The Huechulafquen Formation (Turner, J.C., 1965a, 1965b, 1976) is composed of intrusive igneous rocks of acid composition with fine porphyric texture, feldspar phenocrysts, microlets filled with calcite and partially altered (chlorite) and ovoid vesicles. This unit belongs to the Choiyoi Magmatic Cycle (Llambías, 1999) established by radiometric ages determined by Schiuma and Llambías (2008) in basement rocks from the near Anticlinal Campamento gas field. During drilling of wells in this area, the existence of highly fractured intervals has been evidenced by the loss of drilling fluid and an increase in mud weight that suggests possible overpressure. A good example of a fractured interval within the basement is observed in the Gu-1092 well, where sidewall rotary core and wireline logs document the andesitic lava of the PreCuyo that supports the granodiorite of the Huechulafquen Formation and the difference between fractured granodiorite and un-fractured rock in the deepest zone (Figure 5).

The petrophysical studies of the sidewall rotary core of the Gu-1092 well show matrix porosity between 1 and 6% porosity. Most of the wells have resistivity and acoustic borehole image logs on which a study of fractures and breakout has been performed to understand the in-situ stress components, natural fracture network and mechanical facies within the basement.

Formation Evaluation

Figure 6 shows the microresistivity image, the resistivities, the total porosity measured by the NMR (MPHS) and the Total Gas for the basement and Precuyano. Because the NMR measures porosity independently of lithology, it is the ideal tool to evaluate the porosity in this type of complex lithologies. The basement has an average of 5% porosity, this being the best measure of storage, that is, the amount of gas present in the reservoir. Observe the influence of gas present in the total gas between X550 and X620 meters, the interval that produces most of the hydrocarbon fluid.

Permeability is generated by natural fractures. A fracture analysis was performed on microresistivity and acoustic image logs, logged simultaneously in water-based mud. Initially, 1675 conductive events were identified on the microresistivity image. In Figure 7 we can observe (track 4) the tadpoles (Cond_Frac) and in track 5 the density of conductive fractures. It is observed that the density of fractures does not show any relationship with the production interval, characterized by the total gas influx. From this initial fracture dataset composed of 1675 events, a subset of fractures was selected, formed by the fractures observed on the resistivity and acoustic image logs. This new dataset has 636 elements and is called Open Fractures (Open_frac). The tadpoles and density of open fractures can be observed in tracks 6 and 7 of Figure 7. A detail of open fractures in well images can be seen in Figure 8. The density of open fractures also shows no correlation with the total gas influx. Fractures in depth are subject to a stress field. To understand the relationship between in-situ stresses and natural fractures, it is necessary to build a geomechanical model. It should be mentioned that natural fractures were generated in the geological past under a stress field that is probably not similar to actual stress field. Stress-related events observed in borehole images, such as breakouts and drilling induced fractures are used to calibrate the geomechanical model (Figure 9).

Naturally fractured reservoirs are often characterized by high-density multi-scale fracture networks, organized in multiple orientation families. However, not all fractures contribute to fluid flow under in situ stress conditions. The Coulomb friction criterion has long been applied to predict the probability of reactivating faults and fractures in the subsurface, and hence quantify which part of the fracture network contributes to flow at in-situ stress conditions (Barton et al, 1997).

Figure 10 presents the geomechanical model indicating a strike fault stress regime (SHmax>Sv>Shmin) modelled using logs and calibrated with borehole image. Once the stress tensor was determined, it was possible to calculate the shear stress/normal stress ratio for each of the fracture surfaces identified on the image and determine the population of fractures whose spatial orientation favors a better hydraulic performance. Fracture analysis identified in the borehole image 636 fractures that were classified as open fractures, in which around 300 are considered critically stressed (Figure 10). These fractures are positioned above the failure line in normal and shear stress space.

The density of critically stressed fractures was computed and compared with observed gas influxes observed during drilling. Critical stress theory suggests that fractures close to localized shear failure are critically stressed and therefore most conductive to fluid flow. Due to enhanced permeability, these fractures can act as fluid conduits between wells or between different reservoir intervals. Evaluation of critically stressed fractures is important for understanding the production mechanisms, placement of injectors/producers, and designing enhanced oil recovery (EOR) programs.

Figure 7 presents in the track 8 the tadpoles of the CSF and track 9 its density. The results show a good correlation between gas influxes in the intervals X550 and X650 meters, the source of the highest well production. These results support the theory that fractures close to localized shear failure are critically stressed and therefore most conductive to fluid flow, presenting higher productivity in this case.

Conclusions

This well was drilled with SE direction with a final inclination angle of 15° (Figure 11). This figure shows the total gas, showing warm colors in the areas with higher gas influxes, present in the upper part of the Vaca Muerta Formation, in the middle part of the Lajas Formation and the basement (intensely fractured level). At this point, it is worth mentioning that the well was drilled with water-based mud with a density less than 1200 gr/lt, which clearly helped to the gas shows in the fractured intervals (Figure 12). Production logs data confirm that most of the production (70% of the production) comes from this heavily fractured interval (Figure 13). The well reached a maximum of stabilized production close to 90 km^3/d of gas with 32 m^3/d of flowback water (Figure 14).

Acknowledgements

We acknowledge to Tigh Reservoirs Management of YPF and Baker Hughes a GE Company for the permission to publish the data of this paper.

References Cited

Aguilera, Roberto: Naturally Fractured Reservoirs, 2nd Edition, PennWell Books, Tulsa, Oklahoma (1995), p.11.

Barton C., Moos D. and Zoback M., 1997. In-situ stress measurements can help define local variations in fracture hydraulic conductivity at shallow depth. The Leading Edge.

Cevallos M., 2011. Rasgos transcurrentes de la Dorsal de Huincul. Geología de la Dorsal de Huincul (S11), XVIII Congreso Geológico Argentino, Neuquén.

Llambías E., 1999. El magmatismo gondwánico durante el Paleozoico Superior–Triásico, en Las Rocas Igneas Gondwánicas, Geología Argentina. Instituto de Geología y Recursos Minerales, Buenos Aires, Anales 29 (14): 349-376.

Schiuma, M. y Llambías, E.J. 2008. New ages and chemical analysis on Lower Jurassic volcanism close to the Huincul High, Neuquén. Revista de la Asociación Geológica Argentina 63: 644- 652.

Silvestro, J y M. Zubiri, 2008, Convergencia oblicua: modelo estructural alternativo para la dorsal Neuquina (39ºs) – Neuquén, Rev. Asoc. Geol. Argent. v.63 n.1, Buenos Aires.

Turner, J. C. M., 1965a. Estratigrafía de la comarca de Junín de los Andes. Academia Nacional de Ciencias, Boletín 44, 5-51. Córdoba.

Turner, J.C.M., 1965b. Estratigrafía de Aluminé y adyacencias (Provincia del Neuquén). Revista de la Asociación Geológica Argentina, 20 (2), 153-1164. Buenos Aires.

Turner, J.C., 1976. Descripción de la Hoja 36 a, Aluminé, provincia del Neuquén. Servicio Geológico Nacional, Boletín 145: 1-80. Buenos Aires.

Zoback, M.D., 2010. Reservoir Geomechanics. Cambridge University Press; 1 edition (May 17, 2010). ISBN-13: 978-0521146197

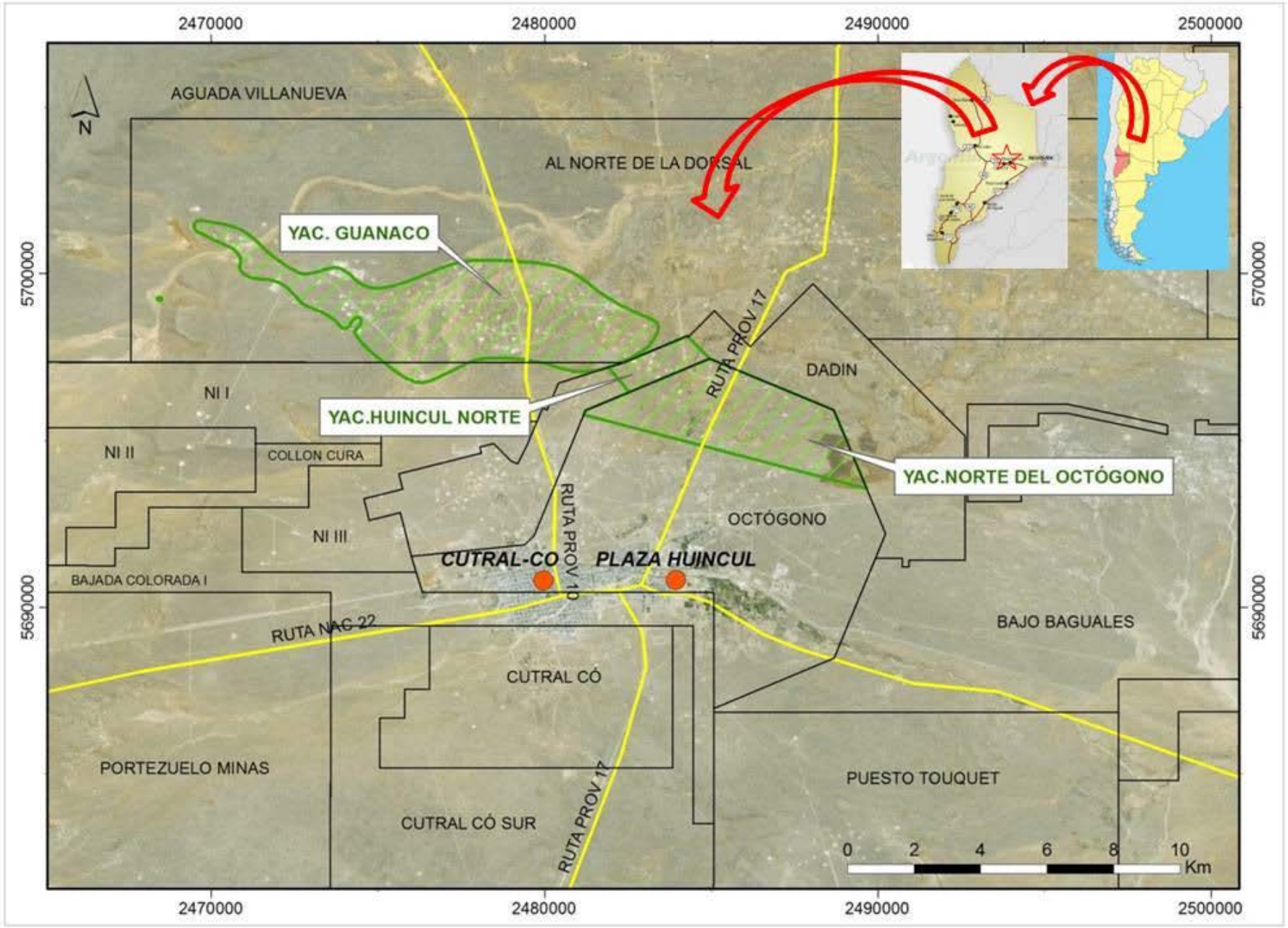

Figure 1. Map of project location with geographical structural continuity of Guanaco to the Huincul Norte and Norte de Octógono projects.

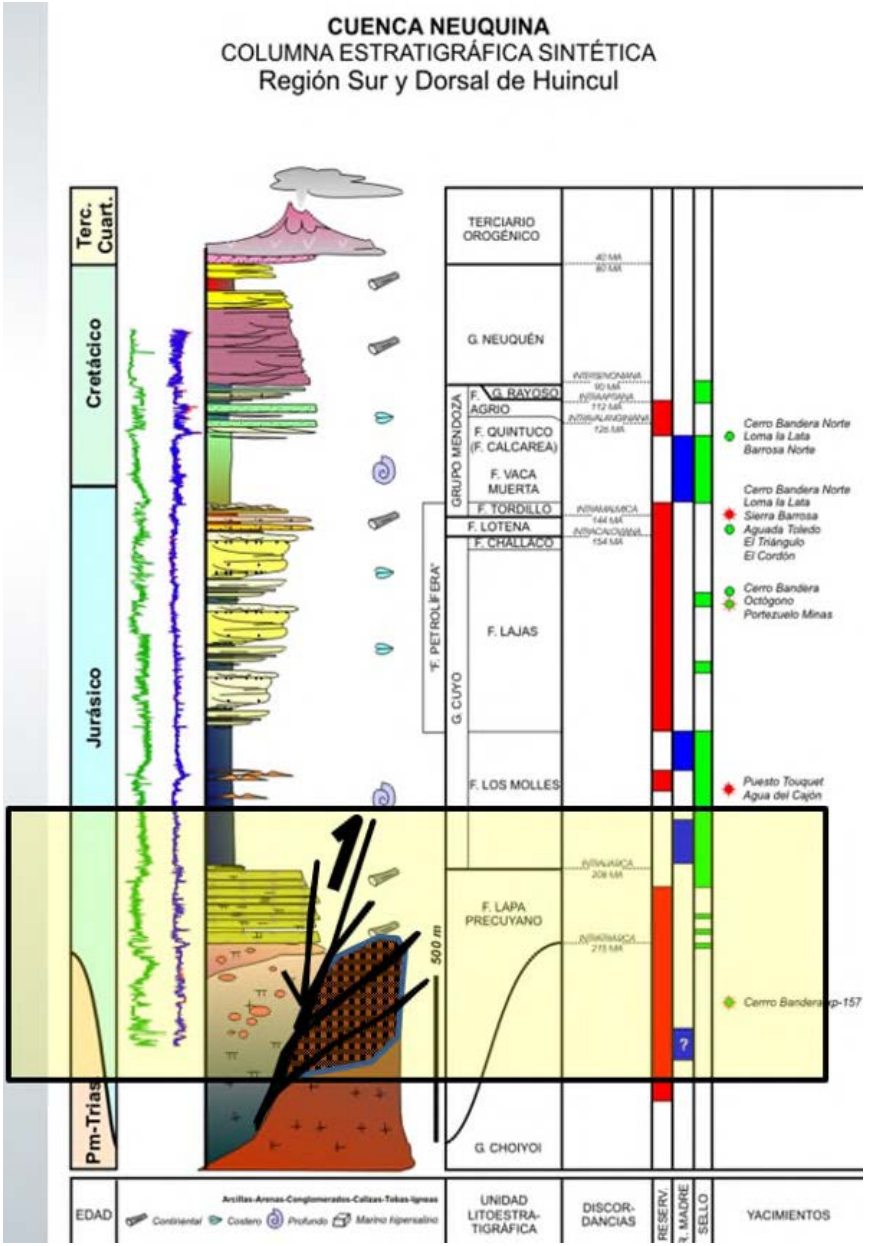

Figure 2. Stratigraphic column, highlighting the main reservoirs and the source rock formations, and the importance of fracturing the basement by tectonics (modified by Brisson 2001).

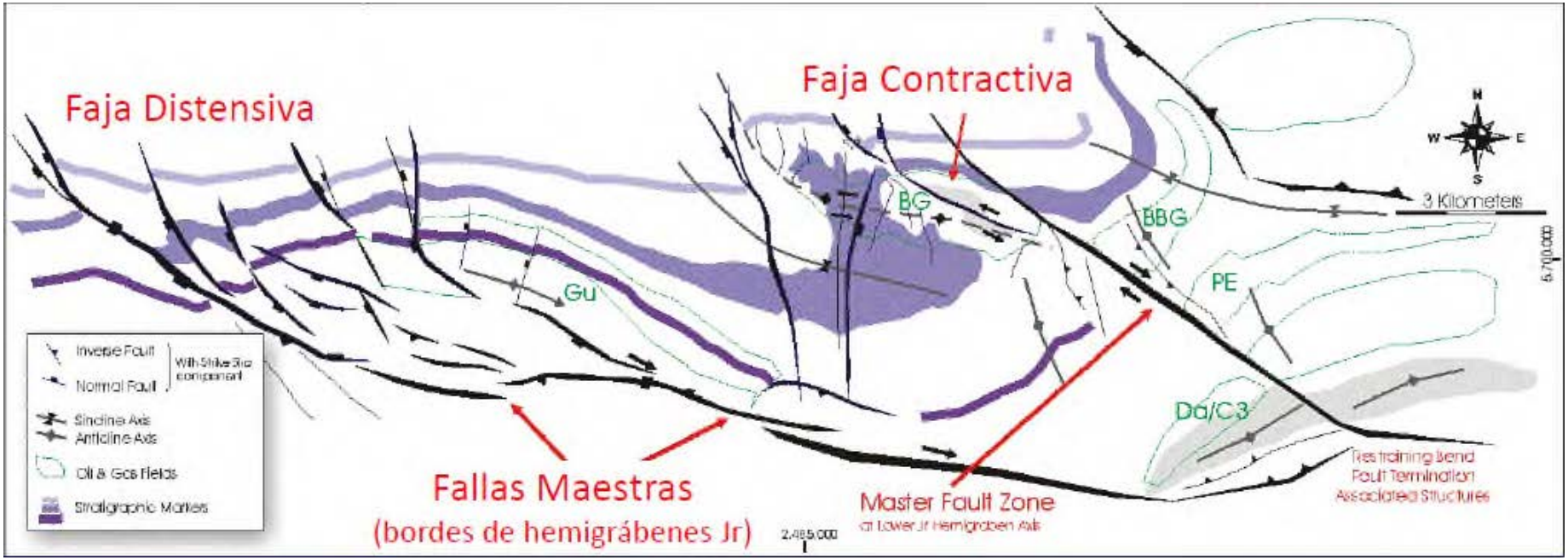

Figure 3. Structural map of the study area (by Cevallos 2011).

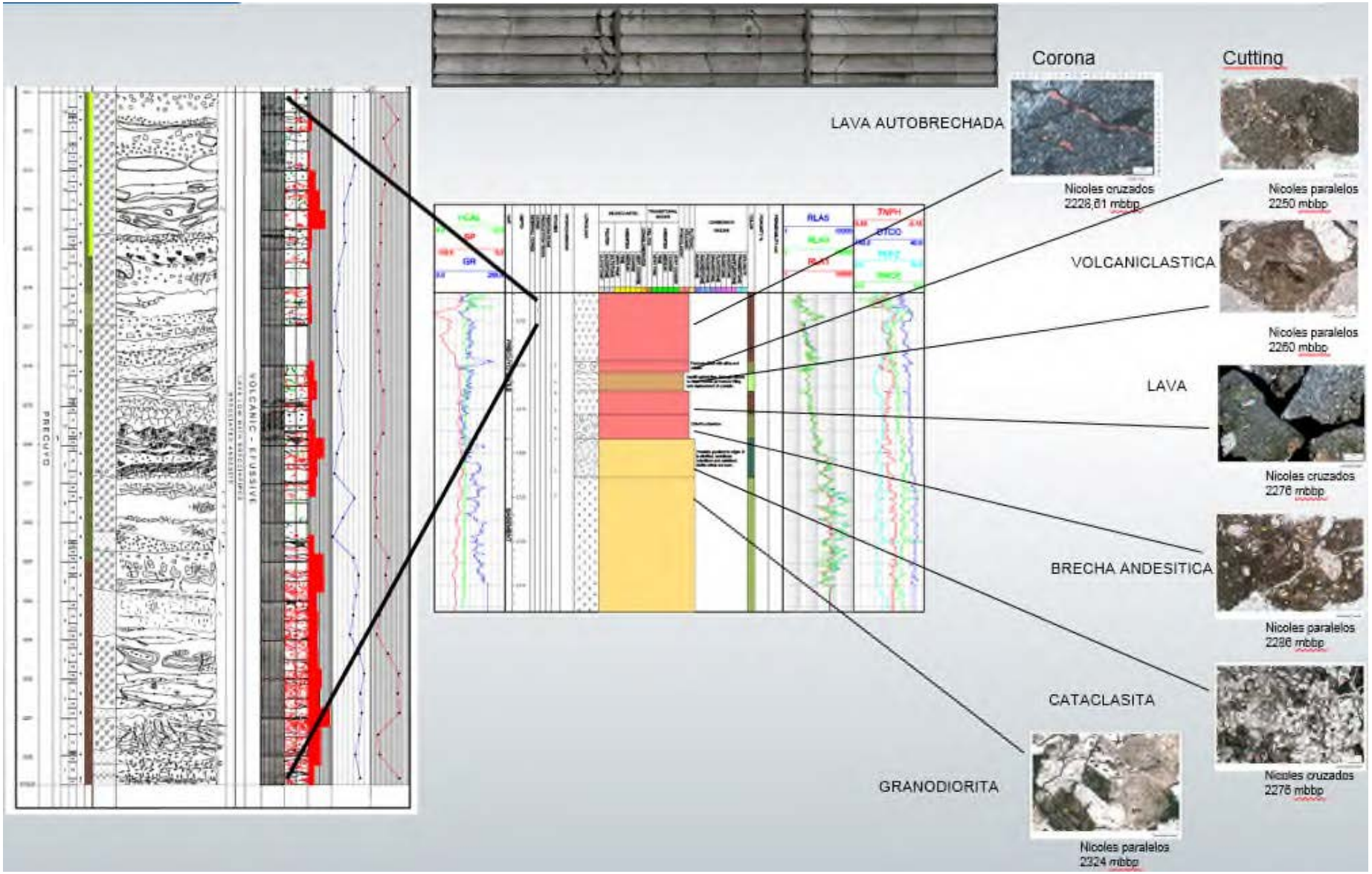

Figure 4. Core and thin sections of cutting of PreCuyo (Gu-1093 well).

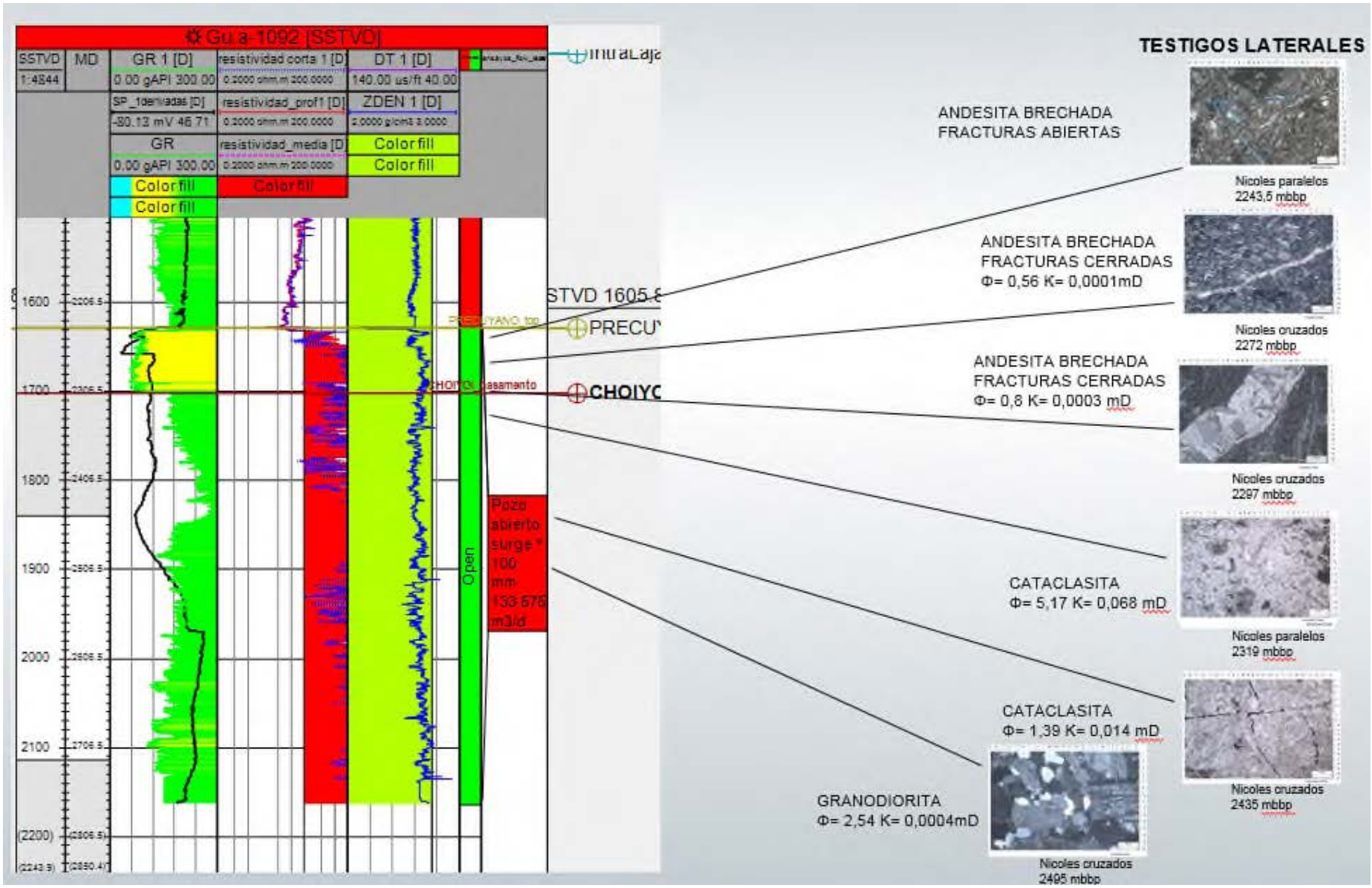

Figure 5. Thin sections of cutting (Gu-1092 well).

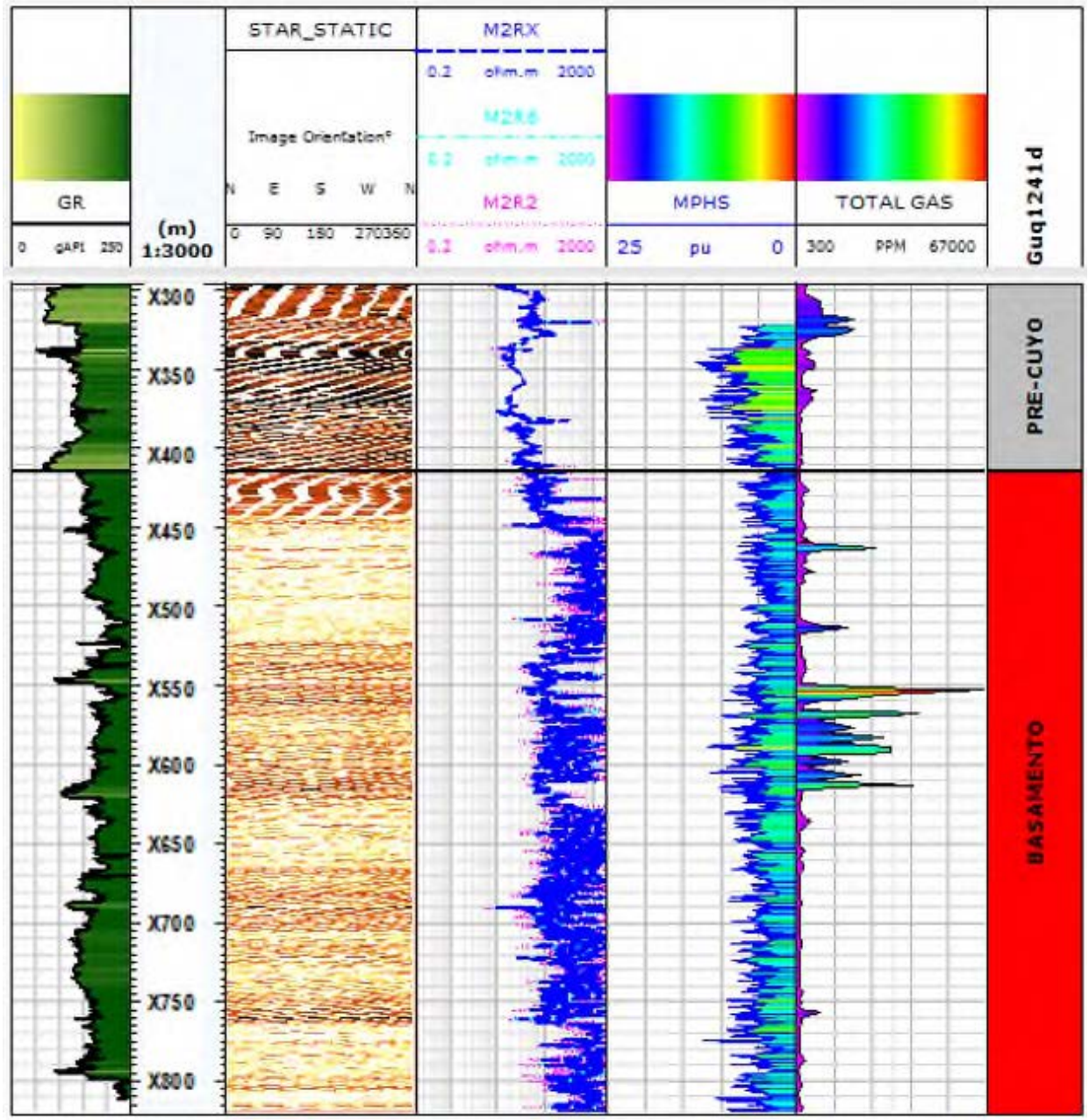

Figure 6. Resistivity and Total Porosity of NMR vs. Total Gas (Basement and Precuyo).

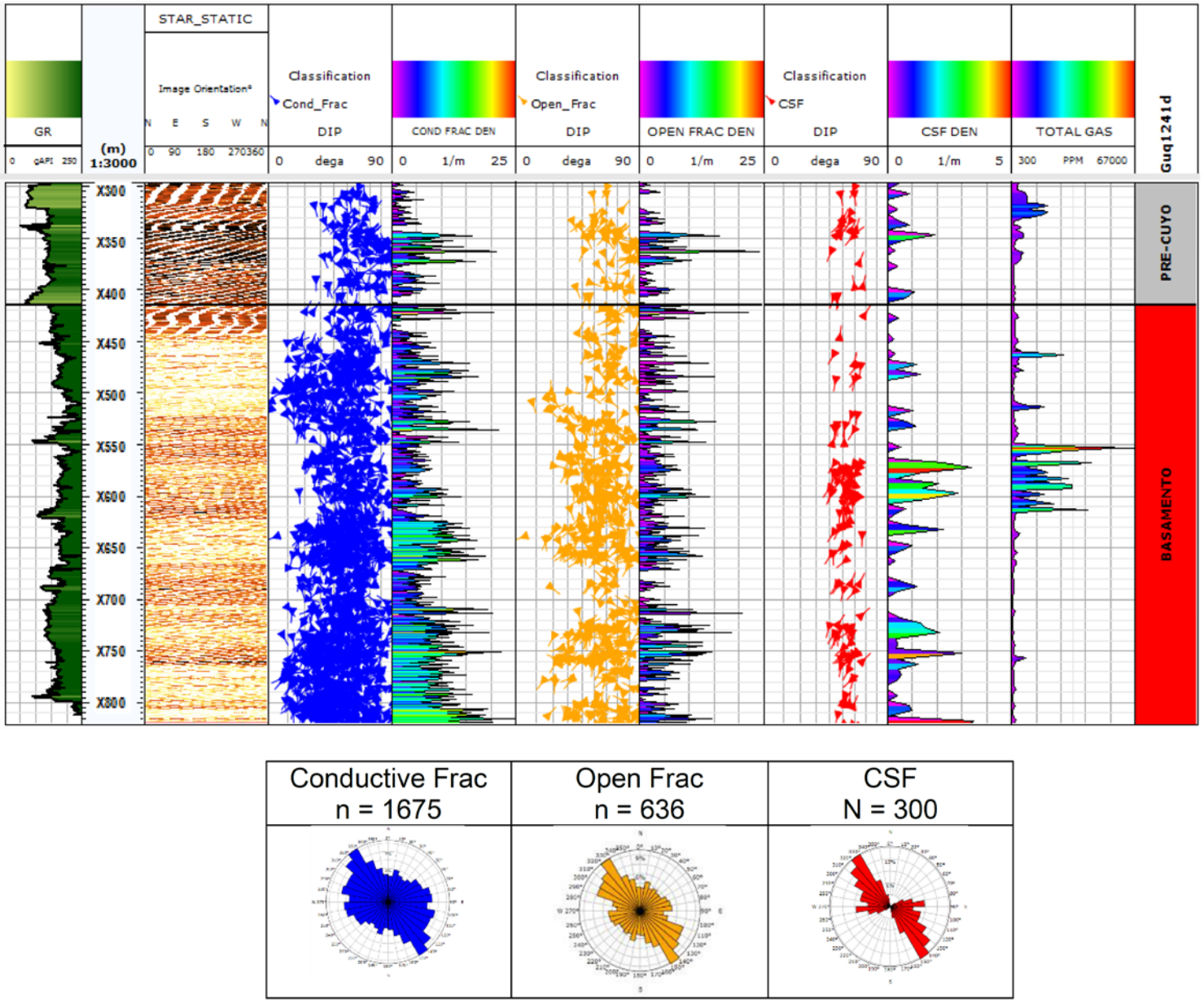

Figure 7. Comparison of conductive, open and critically stressed fractures (tadpoles and compensated fracture density) and Total Gas. Rose plots of the different datasets of identified fractures.

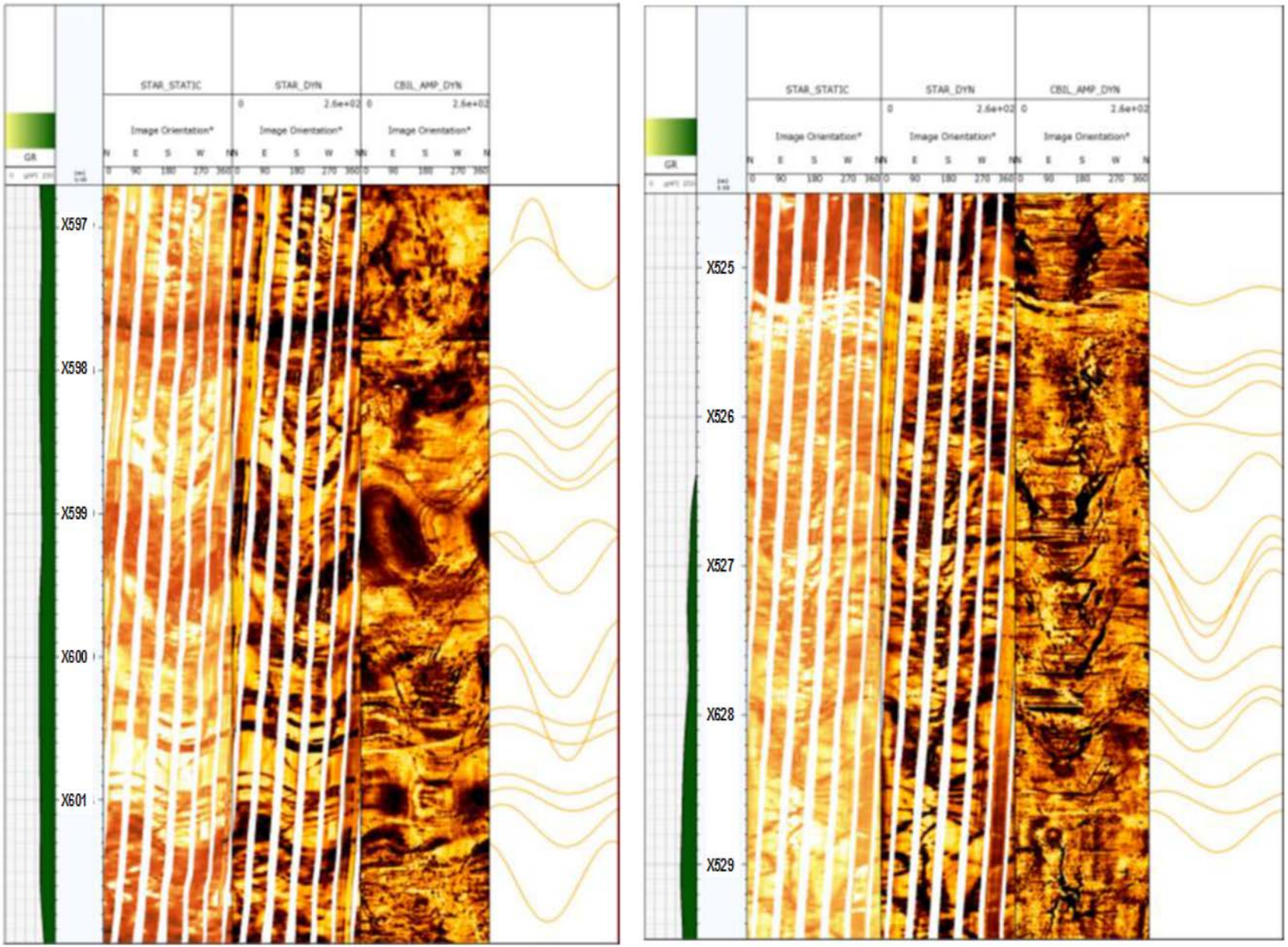

Figure 8. Detailed Identification of open fracture system observed in the microresistivity borehole images (tracks 4 and 5) and acoustic (track 5).

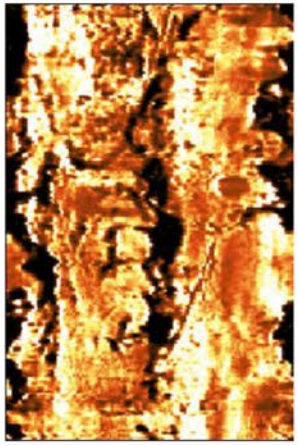

Breakout

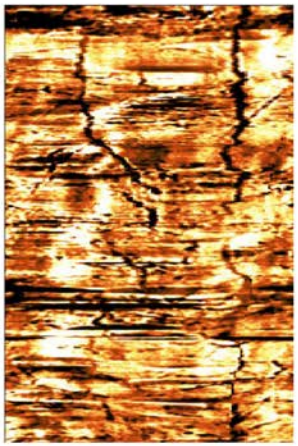

DIF (Drilling Induced Fractures)

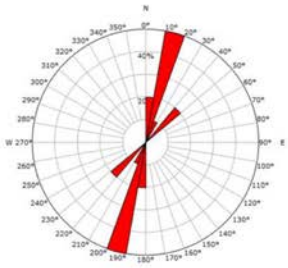

Breakout
N°: 10
NNE-SSW
Sh: 20°

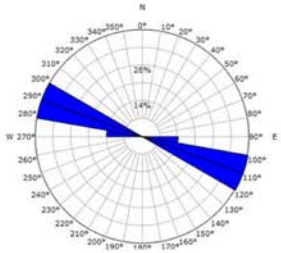

DIF
N°: 07
WNW-ESE
SH: 110°

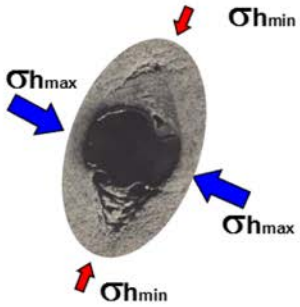

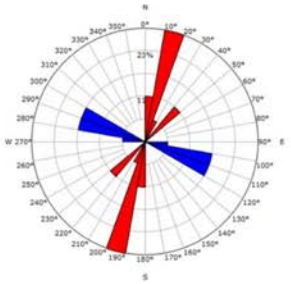

Breakout and DIF relationship

Figure 9. Breakouts and DIF and its relationship with the in-situ stress field.

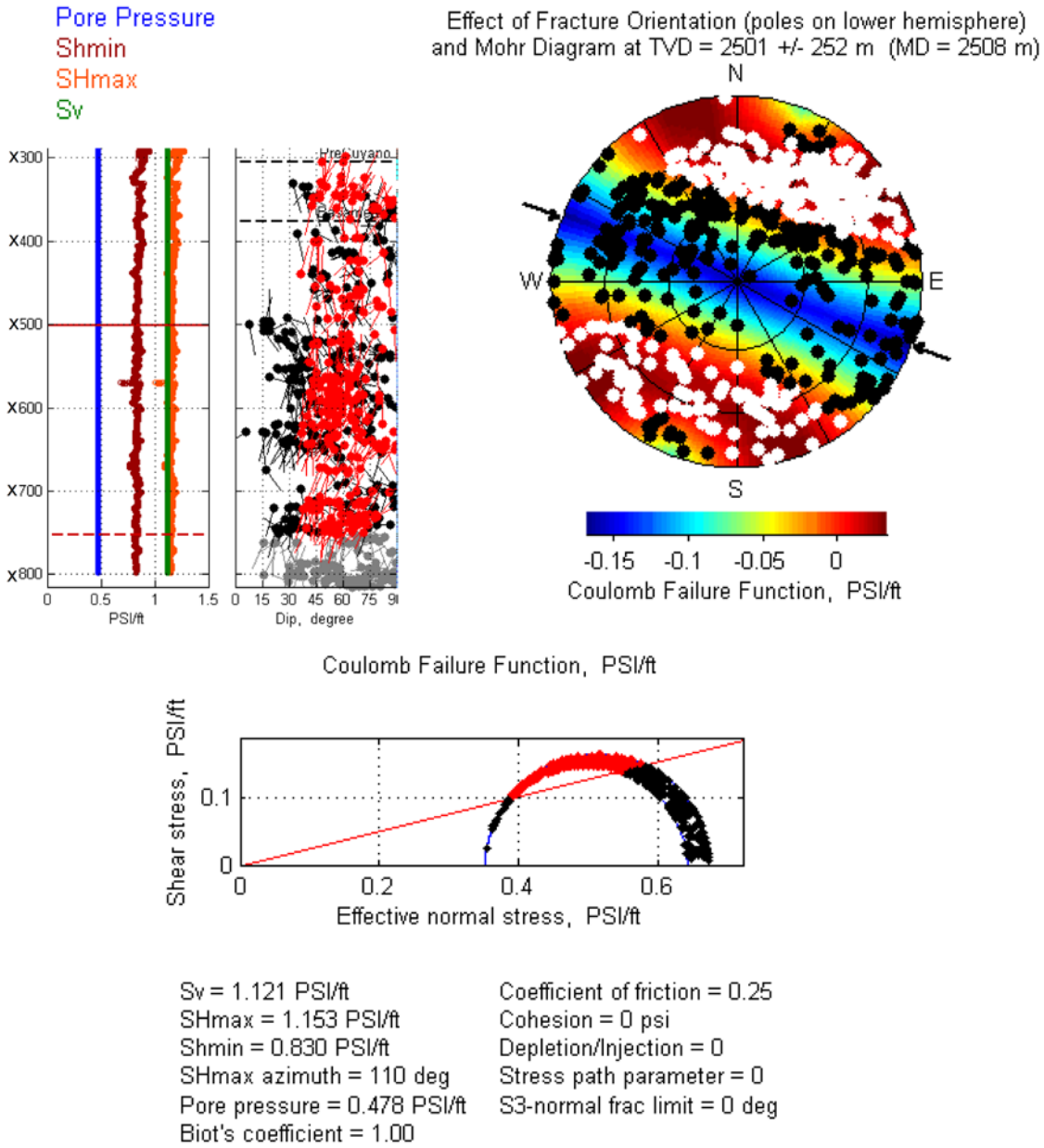

Figure 10. Geomechanical Model, Fracture Model and Evaluation of Critically Stressed Fracture (red fractures, left and bellow; white fractures in right side).

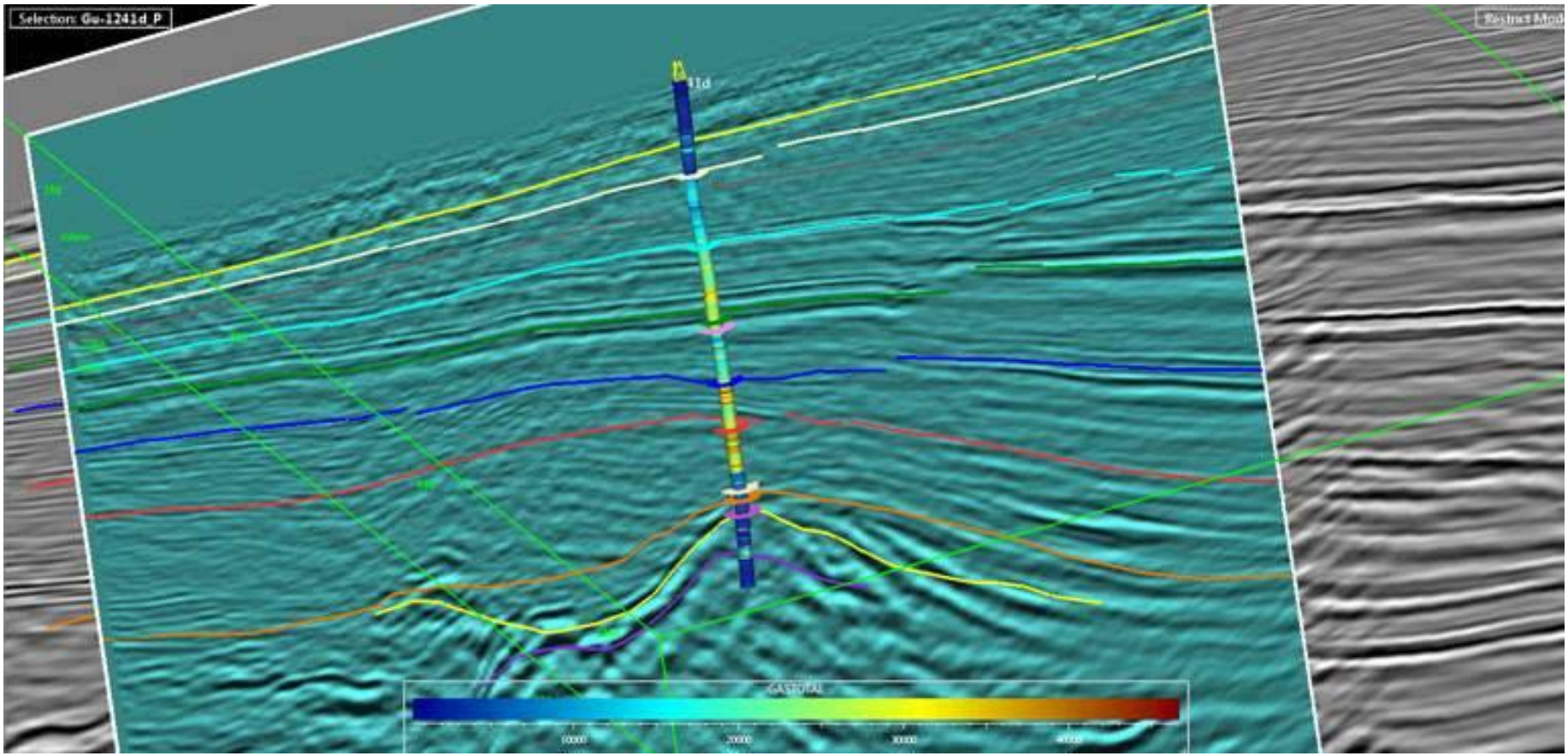

Figure 11. Trajectory of the well drilled inside a cube of amplitude and in the cube of relative impedance, both in depth. Gas scale 0 to 50000 ppm (cold to hot colors).

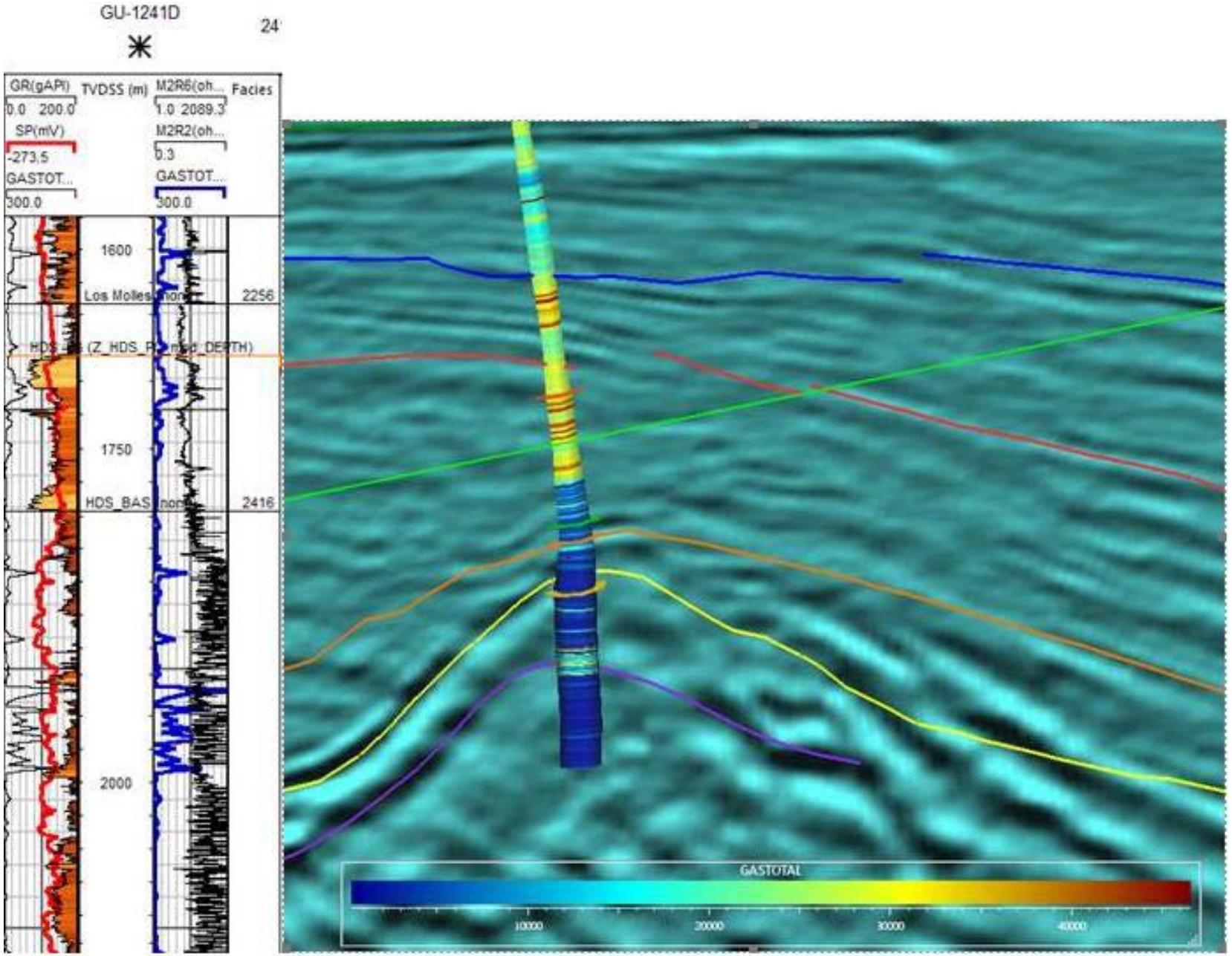

Figure 12. Open hole logs adjustment with relative impedance cube. Gas scale 0 to 50000 ppm (cold to hot colors).

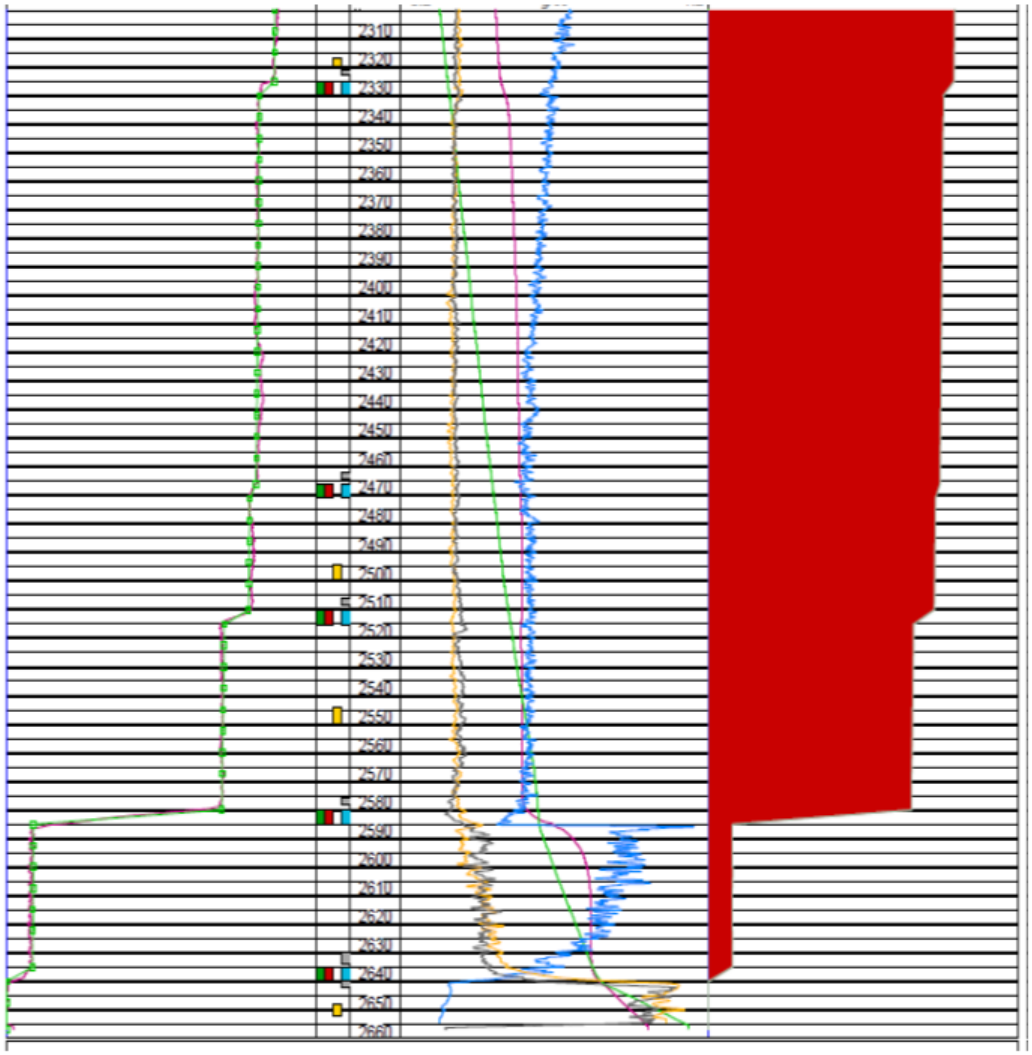

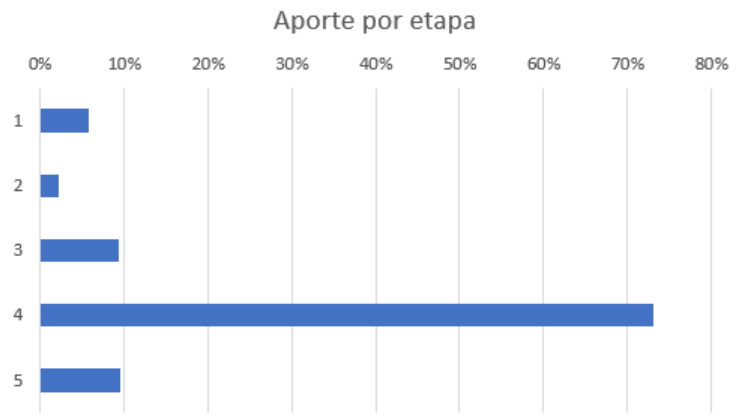

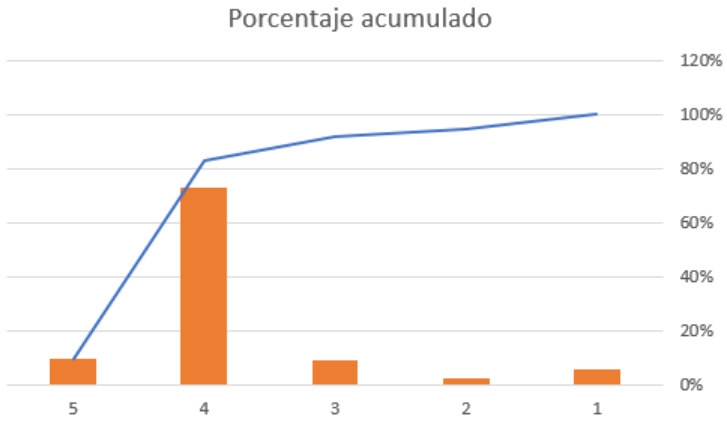

Figure 13. PLT shows the contribution per layer of the 5 layers fractured hydraulically. Stage 4 correspond to maximum gas total influx during drilling.

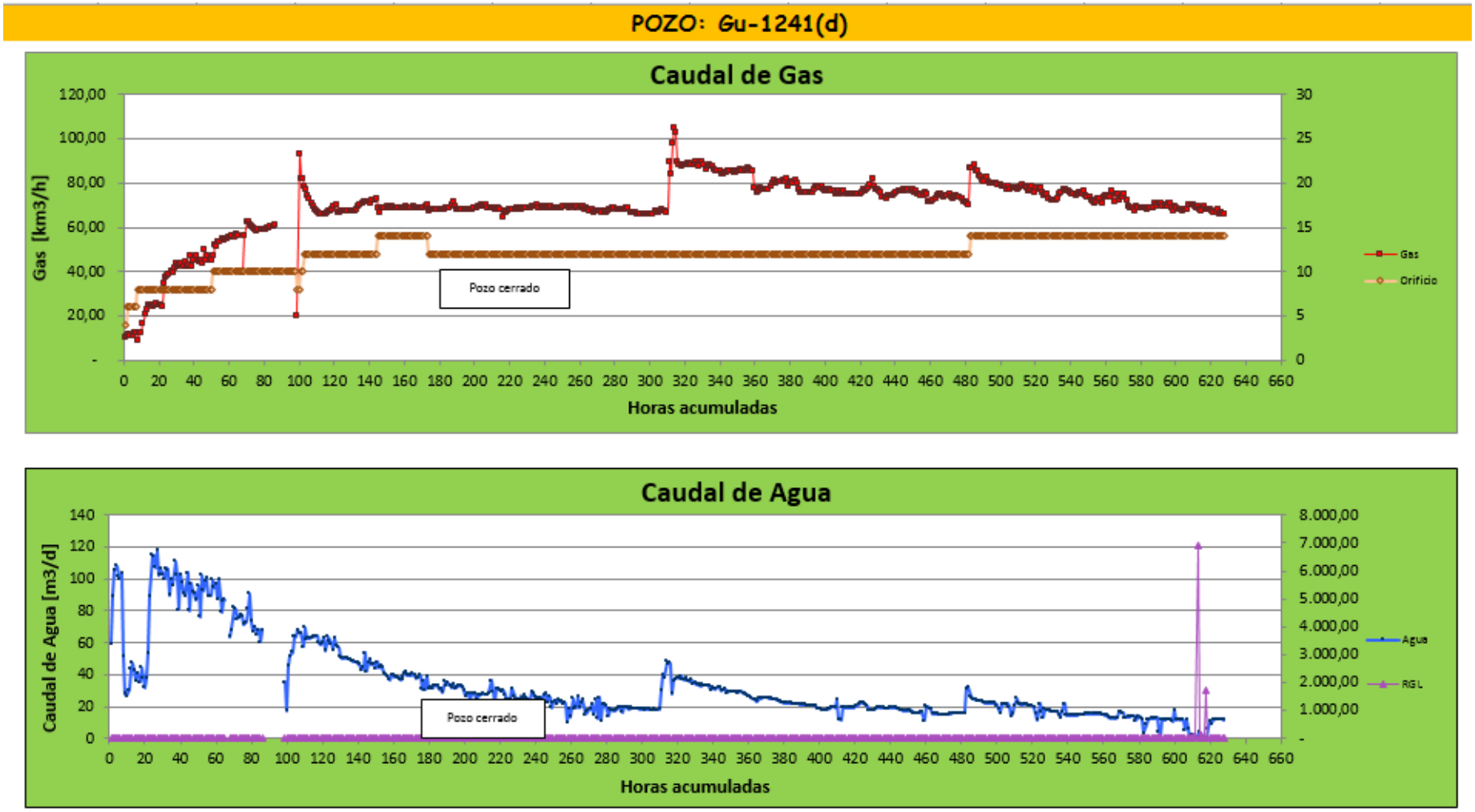

Figure 14. Production of gas from well Gu-1241d during the flowback test at different chokes.